ADVANCED BIOSYSTEMS
www.adv-biosys.com

Rapid, Point-of-Care, Paper-Based Plasmonic Biosensor for Zika Virus Diagnosis

Qisheng Jiang, Yatin J. Chandar, Sisi Cao, Evan D. Kharasch, Srikanth Singamaneni, and Jeremiah J. Morrissey**

Zika virus (ZIKV) is an increasing global health challenge. There is an urgent need for rapid, low-cost, and accurate diagnostic tests that can be broadly distributed and applied in pandemic regions. Here, an innovative, adaptable, and rapidly deployable bioplasmonic paper-based device (BPD) is demonstrated for the detection of ZIKV infection, via quantification of serum anti-ZIKV-nonstructural protein 1 (NS1) IgG and IgM. BPD is based on ZIKV-NS1 protein as a capture element and gold nanorods as plasmonic nanotransducers. The BPD displays excellent sensitivity and selectivity to both anti-ZIKV-NS1 IgG and IgM in human serum. In addition, excellent stability of BPDs at room and even elevated temperature for one month is achieved by metal–organic framework (MOF)-based biopreservation. MOF-based preservation obviates the need for device refrigeration during transport and storage, thus enabling their use in point-of-care and resource-limited settings for ZIKV surveillance. Furthermore, the versatile design (interchangeable recognition element) of BPDs more generally enables their ready adaptation to diagnose other emerging infectious diseases.

1. Introduction

ZIKV virus (ZIKV), a mosquito-borne Flavivirus, has become a global public health challenge.[1] ZIKV can cause congenital Zika syndrome in newborns and Guillain–Barré syndrome in adults and has raised a grave concern.[2] Unfortunately, ZIKV-infected individuals are largely asymptomatic or have mild symptoms, which are very similar to other mosquito-borne Flavivirus infections.[3] However, most current diagnostic techniques take days and a central laboratory to obtain results. These techniques are relatively expensive, require equipment that is not amenable to remote, and resource-limited regions such as refrigeration and bench-top plate readers where disease surveillance and control are critically needed.[4] Thus, there is a need for rapid, inexpensive, and accurate testing for ZIKV in point-of-care (POC) and resource-limited settings not dependent on refrigeration for test integrity. Additionally, an inexpensive, rapid test allows retention of infected individuals to affect immediate treatment and for counseling of pregnant women and women of childbearing age.

ZIKV nonstructural protein 1 (NS1) is necessary for viral replication and involved in immune evasion, viral pathogenesis[3] and is a major antigenic marker for ZIKV infection detectable for 1–2 weeks.[5] An ensuing host IgM/IgG response to ZIKV-NS1 (which evolves within one week) can serve as the basis of diagnostic assays for ZIKV infection providing a detection window of several months. Despite having high structural similarity with other Flavivirus NS1 proteins, ZIKV-NS1 displays a loop-surface interface with divergent electrostatic potential, avoiding cross reactivity with Dengue virus and other Flavivirus NS1 proteins, which can be exploited to differentiate ZIKV from other Flavivirus infections.[6]

Plasmonic biosensors based on refractive index sensitivity of localized surface plasmon resonance (LSPR) are highly promising for sensitive and cost-effective biodiagnostics.[7] LSPR of metal nanostructures is shown to be sensitive enough to differentiate various inert gases (refractive index difference on the order of 3×10^{-4} refractive index units), probe the conformational changes of individual biomacromolecules, detect single biomolecule binding events, monitor the kinetics of catalytic activity of single nanoparticles, and even optically detect a single electron.[8]

We have previously introduced bioplasmonic paper device (BPD) as a novel platform for implementing LSPR-based biosensors.[9] Compared with conventional rigid substrates such as silicon and glass, paper substrates offer numerous advantages such as high surface area, excellent wicking properties, mechanical flexibility, low cost, easy disposability, small sample

Q. Jiang, S. Cao, Prof. S. Singamaneni
Department of Mechanical Engineering and Materials Science
Institute of Materials Science and Engineering
Washington University in St. Louis
Saint Louis, MO 63130, USA
E-mail: singamaneni@wustl.edu
Y. J. Chandar
The Davidson Academy of Nevada
Reno, NV 89507, USA
Prof. E. D. Kharasch, Prof. J. J. Morrissey
Department of Anesthesiology
Siteman Cancer Center
Washington University in St. Louis
St. Louis, MO 63110, USA
E-mail: morrisseyjj@wustl.edu
Prof. E. D. Kharasch
Department of Biochemistry and Molecular Biophysics
Washington University in St. Louis
St. Louis, MO 63110, USA

DOI: 10.1002/adbi.201700096

volume requirement, facile processing (cutting, bending, and dipping), and compatibility with conventional printing approaches (enabling multiplexed detection and multimarker biochips). Simply involving conventional laboratory filter paper adsorbed with biofunctionalized nanostructures, BPD exhibit great potential for the use of label-free, POC bioassays with the combination of handheld, battery-operated spectrometers. More importantly, with interchangeable recognition elements, BPD can be swiftly adapted for molecular diagnosis of many other diseases.

Recently, we introduced a simple and highly effective technique based on a zeolitic imidazolate framework-8 (ZIF-8) layer for preserving the biorecognition capability of immobilized antibodies at ambient and elevated temperatures for several days.[10] This facile and low-cost biopreservation method will allow the on demand use of paper-based plasmonic sensors in point-of-care and resource-limited settings without the need for "cold chain" refrigeration, especially in tropical areas, where ZIKV monitoring and containment are of paramount importance[11]

Here, we introduce a rapid, point-of-care, low-cost assay based on BPDs for ZIKV diagnosis that can be employed in resource-limited regions. ZIKV-NS1 protein was used as the recognition element for the capture and detection of anti-ZIKV-NS1 IgG and IgM; recognized diagnostic biomarkers of ZIKV infection.[6] BPDs exhibited excellent spectral homogeneity, sensitivity, dynamic range, selectivity, and importantly, effective detection in validated ZIKV patients' sera. Finally, coupled with metal–organic framework (MOF)-based biopreservation method, ZIKV paper-based plasmonic sensors exhibited excellent recognition ability after storage at room and elevated temperature for one month, indicating great potential for application in resource-limited regions without the need of cold chain transport/storage.

2. Results and Discussion

2.1. Preparation of ZIKV-Based BPDs

The detection of antibodies against ZIKV-NS1 protein can be used as an accurate diagnostic approach due to the highly specific immune-response ensued by ZIKV-NS1 protein.[6e] We employed full length recombinant ZIKV-NS1 protein (M_w = 43 kDa, MyBiosource, San Diego, CA) as the recognition element and a monoclonal anti-ZIKV-NS1 IgG (My Biosource) as the target bioanalyte to demonstrate the BPD. Because of their large refractive index sensitivity and excellent tunability of the LSPR wavelength,[12] gold nanorods (AuNRs) were employed as plasmonic nanotransducers (**Figure 1**).

We synthesized AuNRs using a seed-mediated method with a length of 63.1 ± 2.6 nm and a diameter of 25.0 ± 1.8 nm (**Figure 2**A and Figure S1, Supporting Information). To conjugate the AuNRs with ZIKV-NS1, we used carbodiimide crosslinker chemistry and thiol-terminated bifunctional polyethylene glycol (SH-PEG) as described earlier (see the Experimental Section for details).[9a,b,13] The SH-PEG-ZIKV-NS1 conjugate covalently bound to the AuNRs surface via an Au–S linkage.[14] The flexible PEG chain increases the accessibility of ZIKV NS1 to target anti-ZIKV-NS1 IgG and also forms a protein-resist layer to reduce nonspecific binding of serum proteins, thus minimizing the assay background. The successful coupling of SH-PEG-ZIKV-NS1 to AuNR in solution resulted in a redshift of ≈2 nm in the longitudinal LSPR wavelength (Figure 2B). Dynamic light scattering (DLS) was employed to monitor changes in the hydrodynamic size of the AuNR after bioconjugation with ZIKV-NS1 (Figure 2C). The increase in hydrodynamic size of about 3 nm indicated the successful appendage of ZIKV-NS1 protein to the AuNRs.

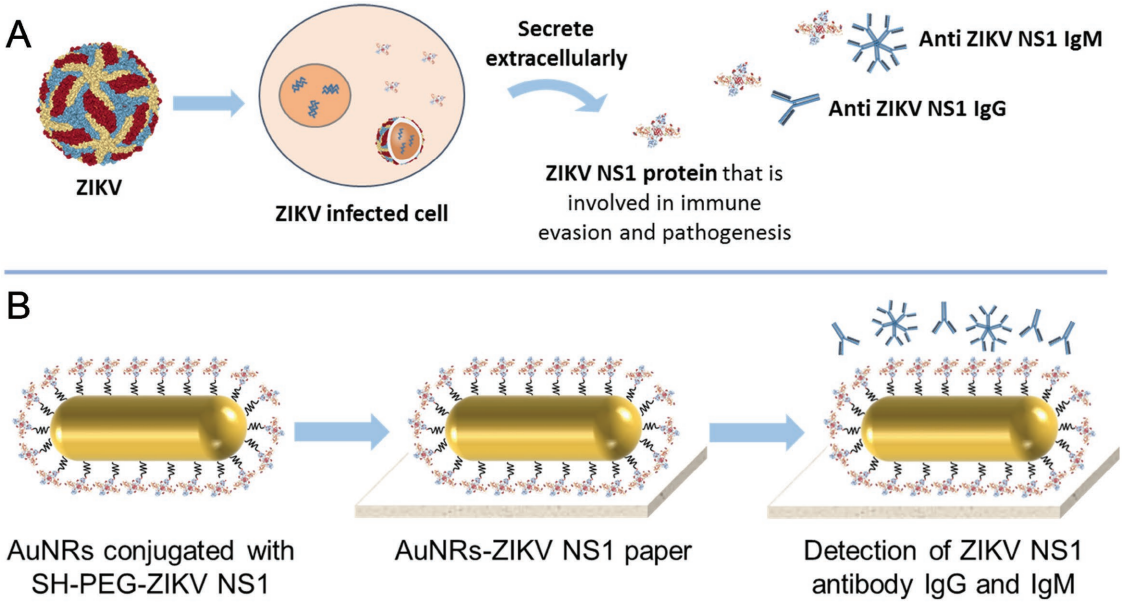

Figure 1. Schematic of BPD design. A) The IgG/IgM response to ZIKV-NS1 protein. B) Illustration of using ZIKV-NS1 protein as recognition element and AuNR as plasmonic transducer to detect anti-ZIKV-NS1 IgG/IgM by BPD (ZIKV illustration obtained from Protein data bank, 5IRE).

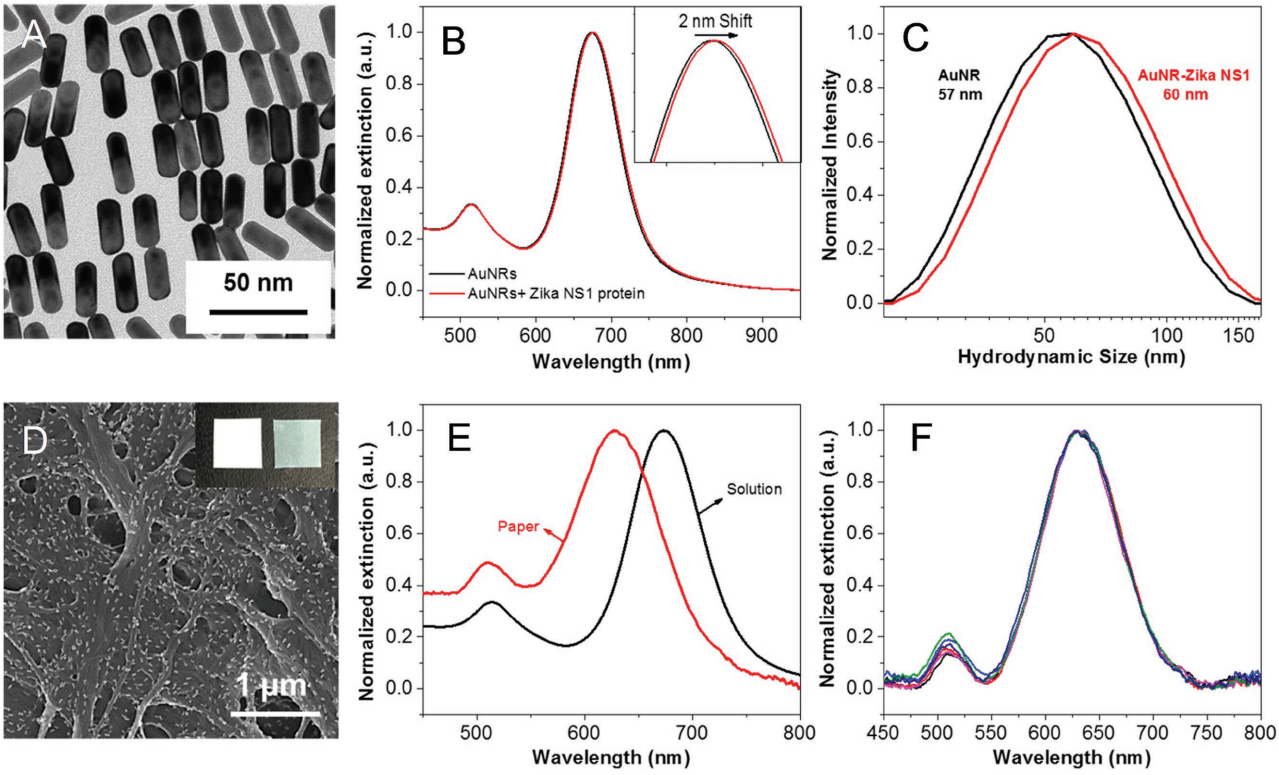

Figure 2. Preparation of ZIKV-NS1-based BPD. A) TEM image of AuNRs. B) UV–vis extinction spectra of AuNRs solution before and after ZIKV-NS1 conjugation. C) Hydrodynamic size obtained from DLS confirming the successful conjugation of ZIKV-NS1 protein on AuNRs surface. D) SEM image of paper absorbed with AuNR-ZIKV-NS1 conjugates (inset shows optical images of the pristine filter paper and filter paper with AuNR-ZIKV-NS1 conjugates). E) Extinction spectra of AuNR-ZIKV-NS1 conjugates solution and on paper. F) Multiple extinction spectra collected from different regions on a ZIKV-NS1-based BPD of 0.5 × 0.5 cm^2 demonstrating the homogeneity of the LSPR wavelength across the sample.

Preparation of BPD was achieved by the immersion of a 1 × 1 cm^2 strip of laboratory filter paper (Whatman #1) in the ZIKV-NS1 functionalized AuNR solution. The scanning electron microscope (SEM) images of the paper revealed a uniform distribution of the AuNR-ZIKV-NS1 conjugates with no signs of aggregation or patchiness (Figure 2D). Longitudinal LSPR wavelength of AuNR-ZIKV-NS1 conjugates adsorbed on paper substrate exhibited a significant blueshift (≈34 nm) compared to that in solution due to the change in the refractive index of the surrounding medium (aqueous to air + substrate) (Figure 2E). Extinction spectra collected at ten different sites across the 0.5 × 0.5 cm^2 area of a BPD revealed excellent optical uniformity of the paper-based plasmonic sensor exhibited a small standard deviation of ≈1 nm (Figure 2F). The excellent spectral homogeneity is due to the highly uniform adsorption of AuNR-ZIKV-NS1 conjugates as evidenced by the SEM images (Figure 2D). The spectral homogeneity observed here is quite remarkable considering the simplicity of the fabrication process and the inherent heterogeneity of the paper substrates (large surface roughness and hierarchical nature of the fibrous mat) compared to the size of the AuNRs themselves.

2.2. Biosensor Performance

To probe the biosensing capability of the BPDs, we exposed them to phosphat buffered saline (PBS) buffer (pH 7.4) spiked with the monoclonal antibody, anti-ZIKV-NS1 IgG. Extinction spectra were obtained from BPDs adsorbed with AuNR-ZIKV-NS1 conjugates and subsequently exposed to anti-ZIKV-NS1 IgG (**Figure 3**A). The LSPR wavelength of BPD exposed to anti-ZIKV-NS1 (100 μg mL^{-1}) on paper exhibited a ≈11 nm redshift compared to pristine AuNRs-ZIKV-NS1 conjugates. To probe the limit of detection, BPDs were exposed to varying concentrations of monoclonal anti-ZIKV-NS1 IgG. A monotonic increase of LSPR shift with increase in the concentration of monoclonal anti-ZIKV-NS1 IgG can be observed (Figure 3B). The limit of detection of the BPD, which is determined by three times the standard deviation of the LSPR shift observed after exposure to pristine PBS (unspiked), was found to be 1 ng mL^{-1}.

To investigate the biosensing performance of BPDs in complex physiological environment with various interference species, we exposed ZIKV-NS1 functionalized BPDs to anti-ZIKV-NS1 IgG in ZIKV-negative human serum diluted 1–10 in PBS. To further reduce possible nonspecific binding in a complex biofluid such as sera, the BPDs were exposed to SH-PEG-CH_3 (2 mg mL^{-1} in PBS buffer pH 7.4) and 10% human serum albumin (HSA) to block the nonspecific binding sites on the AuNRs on paper substrates (see method for details). LSPR wavelength exhibited a ≈10 nm redshift after the exposure of SH-PEG-CH_3/HSA blocking agents and a further redshift of ≈ 9.5 nm upon exposure of anti-ZIKV-NS1 IgG in diluted (10X in PBS) human serum (Figure 3C). The LSPR

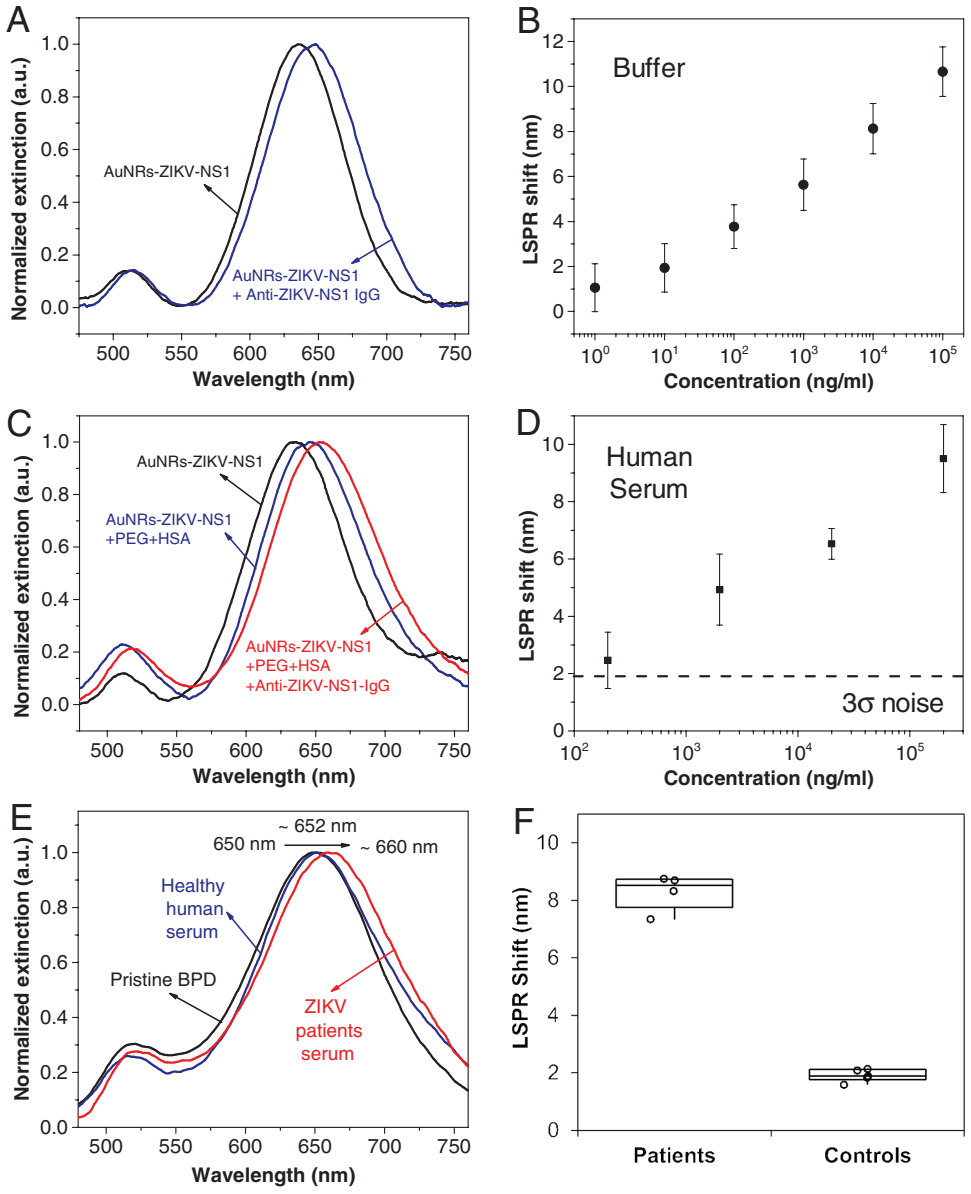

Figure 3. Sensing performance. A) Extinction spectra of ZIKV-NS1-based BPD and ZIKV-NS1-based BPD exposed to buffer spiked with anti-ZIKV-NS1 IgG. B) Anti-ZIKV-NS1 IgG sensing at different concentrations in buffer ($n = 8$ determinations at each concentration). C) Extinction spectra of ZIKV-NS1-based BPD and ZIKV-NS1-based BPD after exposure to PEG/HSA (for blocking nonspecific binding) and ZIKV-NS1-based BPD exposed in 10% human serum spiked with anti-ZIKV-NS1 IgG. D) LSPR shift of the BPD exposed to anti-ZIKV-NS1 at different concentrations in 10% human serum ($n = 8$ determinations at each concentration). E) Extinction spectra of ZIKV-NS1-based BPD exposed ZIKV-negative and ZIKV-positive human serum. F) LSPR peak shift of four ZIKV-positive patients and five ZIKV-negative control sera. The individual results are shown as (O) in a box and whisker plot. The middle line of the box is the median while the top and bottom lines of each box represent the 3rd and 1st quartile values. The lower whisker represents the lowest value while the upper whisker (obscured by a data point) represents the highest value.

shift exhibited a monotonic increase with the increase in the concentration of anti-ZIKV-NS1 IgG in serum (Figure 3D). Note that there is a ≈1.9 nm shift due to nonspecific binding of blood proteins. Thus, the limit of detection of BPDs in serum (200 ng mL^{-1}) is higher compared to that in PBS buffer (1 ng mL^{-1}).

These results demonstrate that BPDs can provide a means for sensitive detection anti-ZIKV-NS1 IgG in complex physiological environments. To further investigate the performance of ZIKV-NS1-based BPDs in clinical applications, we performed bioplasmonic assay on serum from ZIKV patients and ZIKV-negative healthy individuals. BPDs were exposed to serum of four patients with verified ZIKV infection purchased from Antibody Systems Incorporated (Hurst, Texas). The serum of five healthy ZIKV-negative individuals served as control. The LSPR wavelength of healthy controls only showed ≈2 nm redshift possibly due to nonspecific binding of the serum proteins. In the case of ZIKV patient serum samples, we measured a significantly higher LSPR redshift ≈7.3–8.5 nm compared to the healthy controls (Figure 3E,F

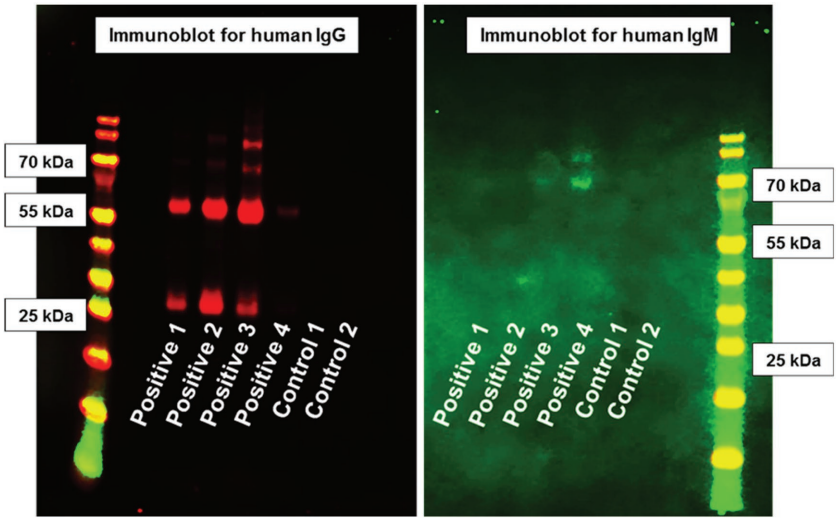

Figure 4. Immunoblot (Western blot) analysis for human IgG (left) and human IgM (right) for ZIKV NS1 protein. SDS sample buffer eluates of the individual ZIKV-NS1-baited bioplasmonic papers were separated by acrylamide gel electrophoresis and immunoblotted for human IgG or IgM as described in the methods. (Left) Bands at 25 and 55 kDa represent human IgG light and heavy chain, respectively. (Right) The band at about 70 kDa represents the human IgM heavy chain.

and Figure S2, Supporting Information) ($p < 0.001$, one-way Analysis of Variance (ANOVA)). Since the concentration curve is semilog, the 2 nm redshift of the control individuals corresponds to ng mL^{-1} equivalents of immunoglobulins while the 7.3–8.5 nm shift of the ZIKV-positive patients is in the range of 100–400 μg mL^{-1} immunoglobulins. That the AuNRs conjugated with ZIKV-NS1 protein captured IgG and IgM from infected patients is shown in **Figure 4**. The diagnostic paper substrates were extensively washed in PBS after the LSPR shift was determined, eluted with sodium dodecyl sulphate (SDS) sample buffer and the eluate analyzed by Western blot. Clearly, the eluates of three ZIKV-positive patients were highly positive for human IgG as indicated by prominent bands at 25 and 55 kDa representing the light and heavy chains of human IgG, respectively, of positive patients 1–3. Positive patient 4 had barely detectable IgG. However, the eluate of patient 4 had a mix of human IgG and human IgM (a prominent band at about 70 kDa representing the heavy chain of human IgM). These findings are consistent with the well annotated information of patient symptoms (all four had joint pain but only three had fever) and results of commercial assays provided by Antibody Systems, Inc. (Hurst, TX) as shown in Table S1 in the Supporting Information. It should be kept in mind that our assay measures the sum of IgG and IgM that bind to the NS1 protein. The eluates of two ZIKV-negative control individuals were undetectable for either immunoglobulin. These results indicate that BPDs can be used for the detection of anti-ZIKV-NS1 IgG and IgM in human serum to differentiate ZIKV-positive from ZIKV-negative individuals.

2.3. Preserving the Biorecognition of the BPDs in the Absence of Refrigeration

The mosquito-borne Flavivirus, ZIKV currently flourishes in mostly resource limited warm and humid regions South and Central America.[11] However, there is concern of ZIKV outbreaks in warm and humid regions of Asia and Africa; equally resource-limited especially with respect to refrigeration. Thus, it is very important for the development and employment of robust bioassays which can remain stable in room and elevated temperature since cold chain transport/storage is greatly lacking. Recently, our group has demonstrated a highly efficient and low-cost method to preserve the activity of antibodies conjugated to plasmonic nanostructures using ZIF-8 as a protective layer.[10] We have employed this novel method to improve the stability of ZIKV-NS1-based BPDs. The LSPR wavelength of BPD can be used to monitor the formation and removal of the ZIF-8 layer (**Figure 5**A,B). The LSPR wavelength exhibited a ≈28 nm redshift after the deposition of ZIF-8 layer (step 2 in Figure 5B and Figure S3A, Supporting Information). After storage of

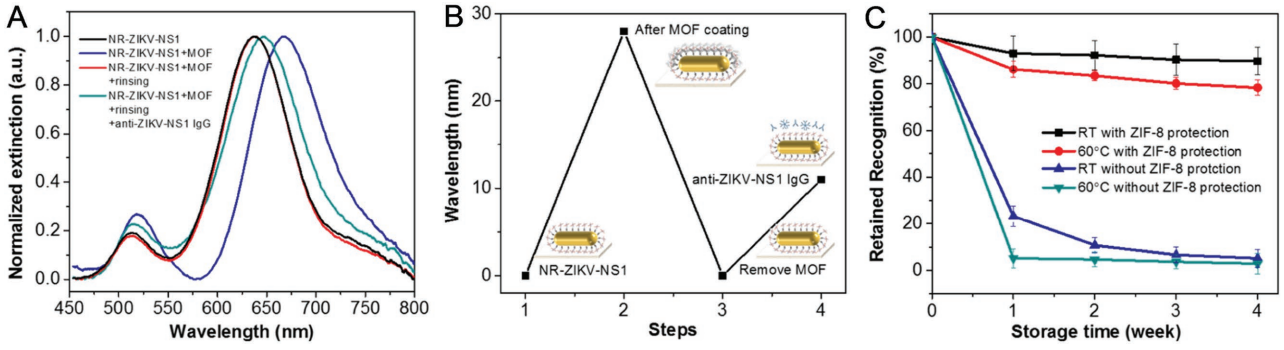

Figure 5. Preservation of ZIKV-NS1-based BPD. A) Extinction spectra of AuNR-ZIKV-NS1 conjugates on paper before and after ZIF-8 protective layer coating, after removing of ZIF-8 film and after exposure to 100 μg mL^{-1} of anti-ZIKV-NS1 IgG. B) LSPR shift corresponding to each step shown in (A). C) Retained recognition capability of MOF-coated ZIKV-NS1-based BPD stored at room temperature (RT) and 60 °C over a span of four weeks ($n = 3$ determinations at each time point). MOF affords significant retention of BPD activity at all time points at both temperatures ($p < 0.001$, one-way ANOVA). MOF affords slight but significant protection at room temperature over 60 °C at 4 weeks ($p = 0.039$, one-way ANOVA with Tukey contrast).

ZIF-8-coated BPD, the protective layer can be quickly removed by washing with distilled water at pH 6 (Figure S3B, Supporting Information). The complete removal of the ZIF-8 layer, which is important to restore the biorecognition capability of BPDs before exposure to target analytes, is evident by a ≈28 nm blueshift in the LSPR wavelength (step 3 in Figure 5B). Subsequently, the LSPR wavelength of restored BPD exhibited a redshift of ≈11 nm upon specific binding of the monoclonal anti-ZIKV-NS1 IgG (200 μg mL^{-1}) to ZIKV-NS1.

To probe the long-term stability of ZIF-8-coated BPDs, we performed a time-lapse experiment to monitor the biorecognition capability of the BPD stored at room temperature and 60 °C for four weeks (Figure 5C and method for details). The ZIKV-NS1-based BPDs with ZIF-8 protective layer retained nearly 89% and 78% of recognition capability after storage at both lab room temperature (herein 20–23 °C) and 60 °C for four weeks. Significantly, bare BPDs without the protective layer quickly lost most of the biorecognition ability at both temperatures compared to the BPDs with the protective MOF layer ($p < 0.001$, one-way ANOVA with Tukey contrast). After four weeks, the room temperature stored had slightly but significantly better activity than those stored at 60 °C ($p = 0.039$, one-way ANOVA with Tukey contrast). These results clearly demonstrate that the ZIF-8 biorecognition preservation method can enable a field-ready BPD, especially in warm, humid regions with epidemic spreading of ZIKV and limited resources.

3. Conclusion

In conclusion, we have developed a rapid, low-cost paper-based plasmonic assay for ZIKV diagnosis. The IgG/IgM response for ZIKV NS1 protein after ZIKV infection is highly specific and has a long-term detection window of several months in infected individuals. The ZIKV-NS1-based BPD displayed excellent sensitivity, specificity, effective detection in validated ZIKV patients' sera, low-cost, and ease of preparation, storage, transport, and disposability. Suitable functionalization of AuNRs with a protein that elicits an immune response (herein ZIKV-NS1) can be used to monitor and quantify the IgM, IgG, and, if present, IgA associated with that immune response.[6e] Combined with the MOF-based biopreservation method, ZIKV-NS1-based BPD holds great potential for providing robust diagnostic solution to current ZIKV outbreak. Furthermore, our versatile BPD platform design can be applied to a broad range of public health threats, allowing for rapid development of low-cost, robust point-of-care diagnostics in resource-limited regions.

4. Experimental Section

Synthesis of Gold Nanorods (AuNRs): Gold nanorods were synthesized using a seed-mediated approach.[15] Seed solution was prepared by adding 0.6 mL of an ice-cold 10×10^{-3} M sodium borohydride solution into 10 mL of 0.1 M cetyltrimethylammonium bromide (CTAB) and 2.5×10^{-4} M chloroauric acid ($HAuCl_4$) solution under vigorous stirring at 25 °C. The color of the seed solution changed from yellow to brown. Growth solution was prepared by mixing 95 mL of CTAB (0.1 M), 0.5 mL of silver nitrate (10×10^{-3} M), 4.5 mL of $HAuCl_4$ (10×10^{-3} M), and 0.55 mL ascorbic acid (0.1 M) consecutively. The solution was mixed by gentle stirring. To the resulting colorless solution, 0.12 mL of freshly prepared seed solution was added and set aside in the dark overnight. Prior to use, the AuNRs solution was centrifuged at 8000 rpm for 10 min to remove excess CTAB and redispersed in nanopure water (18.2 MΩ cm).

AuNRs-ZIKV-NS1 Conjugation: A solution was prepared by adding heterobifunctional polyethylene glycol (SH-PEG-COOH) in water (2×10^{-6} M, M_w = 5000 g mol^{-1}, Jenkem Technology) with the same molar ratio of 1-ethyl-3-(3-dimethylaminopropyl) carbodiimide (Thermo Scientific), and *N*-hydroxy succinimide (Thermo Scientific), followed by shaking for 1 h. The pH of the above reaction was adjusted to 7.4 by adding 10 × concentrated PBS, followed by the addition of 200 μL of recombinant ZIKV-NS1 protein (9.1×10^{-6} M, M_w = 43 kDa). The reaction mixture was incubated for an additional 2 h and concentrated/filtered to remove excess chemicals and byproducts by centrifugation using a microcentrifuge tube with a 30 kDa filter (Amicon Ultra-0.5 concentrator). The conjugate mixture was then washed and reconcentrated in the filter with water twice. The AuNR-ZIKV-NS1 was prepared by adding 30 μL SH-PEG-ZIKV-NS1 conjugate solution (18.2×10^{-6} M) to 1 mL twice centrifuged AuNRs solution with incubation for 1 h.

AuNRs-ZIKV-NS1 Paper Preparation and Tests in Buffer: A regular laboratory filter paper (Whatman #1) was used for the absorption of AuNRs- ZIKV-NS1 conjugates. Typically, a 1 × 1 cm^2 paper strip is immersed in a solution of AuNR- ZIKV NS1 conjugates overnight at 4 °C. The paper strip was taken out and extensively washed with water to remove unbound AuNR-ZIKV-NS1 and any SH-PEG-ZIKV-NS1. The papers can be cut to appropriate size (0.5 × 0.5 or 0.3 × 0.3 cm^2) and immersed in different concentrations of anti-ZIKV-NS1 IgG in PBS buffer (pH 7.4) for 1 h at 4 °C. It was removed and washed thoroughly with PBS buffer (7.4) and dried under a stream of nitrogen.

Spiked Human Serum Test: In the case of testing the spiked human serum, ZIKV-NS1-based BPDs were exposed to 2×10^{-6} M SH-PEG-CH_3 and then 10% human serum albumin solution to saturate any nonspecific binding sites on the AuNRs and paper substrate. The sensor was then washed using PBS buffer (pH 7.4) prior to use. For establishing dose-response curves, anti- ZIKV-NS1 IgG of various concentrations was used to spike human serum (1–10 dilution) in PBS buffer (pH 7.4). The BPDs were immersed in these solutions and left at 4 °C for 1 h, washed thoroughly with PBS buffer, and dried for extinction spectra measurements.

Clinical Test: For testing the capability for clinical samples, the developed BPDs (after nonspecific binding prevention processes mentioned above) were exposed to sera (1–10 dilution) of four ZIKV-positive patients (purchased from Antibody Systems, Inc., Hurst, TX) and five healthy control individuals from the metropolitan St. Louis area (Approval was obtained from the Washington University Institutional Review Board and written informed consent was obtained from all patients) for 1 h and washed thoroughly with PBS buffer, dried for extinction spectra measurements.

ZIF-8 Biorecognition Preservation: To form ZIF-8 films on AuNRs-ZIKV-NS1 paper, 1 mL of 2-methylimidazole solution (160×10^{-3} M, in nanopure water) was mixed with 1 mL of zinc acetate dihydrate solution (40×10^{-3} M, in nanopure water), and agitated for 10 s. The paper was incubated in a freshly made ZIF-8 precursor solution described above for 3 h to facilitate growth of the MOF layer. Subsequently, the paper with and without MOF layer were stored in both room temperature (nominal lab temperature 20–23 °C) and 60 °C for various time and the ability to detect anti-ZIKV-NS1 IgG was tested after rinsing the ZIF-8 layer with nanopure water at pH 6 for 5 min. The percentage of retained recognition capability was used to quantitatively evaluate the antibody preservation efficacy of the MOF under various storage conditions. The retained recognition capability was calculated as the percentage of the redshift upon specific binding of anti-ZIKV-NS1 (100 μg mL^{-1}) to a restored biochip after several days of storage at elevated temperatures compared with the redshift obtained from the same batch of freshly made substrate (which was considered as the reference sample tested

instantly without an MOF coating). For example, the redshift of 10 nm compared with the redshift of 11 nm in the case of the reference sample in the same batch corresponds to a retained recognition capability of 91%.

Characterization Techniques: Transmission electron microscopy (TEM) images were recorded on a JEM-2100F (JEOL) field emission instrument. Samples were prepared by drying a drop of the solution on a carbon-coated grid, which had been previously made hydrophilic by glow discharge. SEM images were obtained using an FEI Nova 2300 Field Emission SEM at an accelerating voltage of 10 kV. The paper was gold sputtered for 60 s before SEM imaging. DLS measurements were performed using Malvern Zetasizer (Nano ZS). Raman spectra were obtained using a Renisha inVia confocal Raman spectrometer mounted on a Leica microscope with 20 x objective and 785 nm wavelength diode laser as an illumination source.

Extinction Spectra Measurements: Extinction spectra from paper substrates were collected using a CRAIC micro-spectrophotometer (QDI 302) coupled to a Leica optical microscope (DM 4000M) with 20 × objective in the range of 450–800 nm with ten accumulations and 100 ms exposure time in reflection mode. The spectral resolution of the micro-spectrophotometer was 0.2 nm. Multiple UV–vis spectra (≈10) were collected from different locations of the paper strip before and after exposure to anti-ZIKV-NS1 IgG solutions. Shimadzu UV-1800 spectrophotometer was employed to collect UV–vis extinction spectra from solution.

Immunoblot: BPD after measurement of the LSPR of patient sera were washed with PBS and eluted with SDS sample buffer. Proteins in the eluate were separated by means of 4–12% acrylamide gels (Invitrogen, CA) and transferred to a nitrocellulose membrane by means of an iBLOT (Invitrogen). The membrane was blocked with a commercial blocking buffer (LI-COR Biosciences, Lincoln, NE) and incubated with 1/500 dilution of mouse antihuman IgM u-chain specific antibody (Sigma-Aldrich, St. Louis, MO) in LI-COR blocking buffer containing 0.05% Tween 20 overnight. After washing in PBS buffer containing 0.05% Tween 20, the membrane was incubated in 1/5000 dilutions each of IRDye 680LT goat antihuman IgG (H + L) and IRDye 800CW goat antihuman IgM u-chain specific antibody diluted in LI-COR block containing 0.05% Tween 20 for 1 h. After extensive washing with PBS buffer containing 0.05% Tween 20, the human IgG and IgM were visualized on an Odyssey Fc Imaging System (LI-COR Biosystems, Lincoln, NE).

Statistical Analysis: Statistical analysis was performed using Analyse-it for Excel 2010 (Analyse-it Software, Ltd, Leeds United Kingdom). A "*P*" value of 0.05 or less was considered significant.

Supporting Information

Supporting Information is available from the Wiley Online Library or from the author.

Acknowledgements

The authors acknowledge support from National Science Foundation (CBET1254399 and CBET 1512043) and funding from the Department of Anesthesiology, Washington University School of Medicine in St. Louis and the Department of Mechanical Engineering and Materials Science, Washington University in St. Louis. The authors thank Nano Research Facility (NRF) at Washington University for providing access to electron microscopy facilities. The authors thank clinical coordinator Marilee Fisher for consenting and obtaining sera from control individuals.

Conflict of Interest

The authors declare no conflict of interest.

Keywords

metal–organic framework, plasmonic sensor, point of care, resource limited settings, Zika virus detection

Received: May 17, 2017
Revised: June 26, 2017
Published online:

[1] World Health Organization, *WHO Director-General Briefs Media on the Zika Situation*, www.who.int/mediacenter/news/statements/2016/zika-update-3-16/en (accessed: October 2016).

[2] a) A. de Oliveira Melo, R. Agular, M. Amorin, M. Arruda, F. de Oliviera Melo, S. Ribeiro, A. Batista, T. Ferreira, M. dos Santos, V. Sampaio, S. Moura, A. Tanuri, *JAMA Neurol.* **2016**, *73*, 1407; b) P. de Oliveira-Szejnfeld, D. Levine, M. Amorim, A. Batista, L. Chimelli, A. Tanuri, R. Agular, G. Malinger, R. Ximenes, R. Robertson, J. Szejnfeld, F. Tovar-Moll, *Radiology* **2016**, *281*, 203; c) T. Dos Santos, A. Rodriguez, M. Almiron, A. Sanhueza, P. Ramon, W. K. de Oliveira, G. E. Coelho, R. Badaro, J. Cortez, M. Ospina, R. Pimentel, R. Masis, F. Hernandez, B. Lara, R. Montoya, B. Jubithana, A. Melchor, A. Alvarez, S. Aldighieri, C. Dye, M. A. Espinal, *N. Engl. J. Med.* **2016**, *375*, 16.

[3] a) M. Atif, M. Azeem, M. R. Sarwar, A. Bashir, *Infection* **2016**, *44*, 695; b) J. Lessler, L. H. Chaisson, L. M. Kucirka, Q. Bi, K. Grantz, H. Salje, A. C. Carcelen, C. T. Ott, J. S. Sheffield, N. M. Ferguson, D. A. Cummings, C. J. Metcalf, I. Rodriguez-Barraquer, *Science* **2016**, *353*, aaf8160; c) L. R. Petersen, D. J. Jamieson, A. M. Powers, M. A. Honein, *N. Engl. J. Med.* **2016**, *374*, 1552.

[4] a) R. deM. Campos, C. Cirne-Santos, G. L. S. Meira, L. L. R. Santos, M. D. de Meneses, J. Friedrich, S. Jansen, M. S. Ribeiro, I. C. da Cruz, J. Schmidt-Chanasit, D. F. Ferreira, *J. Clin. Virol.* **2016**, *77*, 69; b) L. Zammarchi, G. Stella, A. Mantella, D. Bartolozzi, D. Tappe, S. Günther, L. Oestereich, D. Cadar, C. Muñoz-Fontela, A. Bartoloni, J. Schmidt-Chanasit, *J. Clin. Virol.* **2015**, *63*, 32; c) R. S. Lanciotti, O. L. Kosoy, J. J. Laven, J. O. Velez, A. J. Lambert, A. J. Johnson, S. M. Stanfield, M. R. Duffy, *Emerging Infect. Dis.* **2008**, *14*, 1232; d) D. Tappe, J. Rissland, M. Gabriel, P. Emmerich, S. Gunther, G. Held, S. Smola, J. Schmidt-Chanasit, *Eurosurveillance* **2013**, *19*, 20685.

[5] a) M. A. Edeling, M. S. Diamond, D. H. Fremont, *Proc. Natl. Acad. Sci. USA* **2014**, *111*, 4285; b) D. A. Muller, P. R. Young, *Ant. Res.* **2013**, *98*, 192; c) M. Sironi, D. Forni, M. Clerici, R. Cagliani, *PLoS Neglected Trop. Dis.* **2016**, *10*, e0004978.

[6] a) W. C. Brown, D. L. Akey, J. R. Konwerski, J. T. Tarrasch, G. Skiniotis, R. J. Kuhn, J. L. Smith, *Nat. Struct. Mol. Biol.* **2016**, *23*, 865; b) H. Song, J. Qi, J. Haywood, Y. Shi, G. F. Gao, *Nat. Struct. Mol. Biol.* **2016**, *23*, 456; c) X. Xu, H. Song, J. Qi, Y. Liu, H. Wang, C. Su, Y. Shi, G. Gao, *EMBO J.* **2016**, *35*, 2170; d) K. Stettler, M. Beltramello, D. A. Espinosa, V. Graham, A. Cassotta, S. Bianchi, F. Vanzetta, A. Minola, S. Jaconi, F. Mele, M. Foglierini, M. Pedotti, L. Simonelli, S. Dowall, B. Atkinson, E. Percivalle, C. P. Simmons, L. Varani, J. Blum, F. Baldanti, E. Cameroni, R. Hewson, E. Harris, A. Lanzavecchia, F. Sallusto, D. Corti, *Science* **2016**, *353*, 823; e) B. Zhang, B. A. Pinsky, J. S. Ananta, S. Zhao, S. Arulkumar, H. Wan, M. K. Sahoo, J. Abeynayake, J. J. Waggoner, C. Hopes, M. Tang, H. Dai, *Nat. Med.* **2017**, *23*, 548.

[7] a) A. J. Haes, R. P. V. Duyne, *Expert Rev. Mol. Diagn.* **2004**, *4*, 527; b) J. N. Anker, W. P. Hall, O. Lyandres, N. C. Shah, J. Zhao, R. P. Van Duyne, *Nat. Mater.* **2008**, *7*, 442; c) K. M. Mayer, J. H. Hafner, *Chem. Rev.* **2011**, *111*, 3828.

[8] a) M. M. Kathryn, H. Feng, L. Seunghyun, N. Peter, H. H. Jason, *Nanotechnology* **2010**, *21*, 255503; b) J. M. Bingham, J. N. Anker,

L. E. Kreno, R. P. Van Duyne, *J. Am. Chem. Soc.* **2010**, *132*, 17358; c) W. P. Hall, J. Modica, J. Anker, Y. Lin, M. Mrksich, R. P. Van Duyne, *Nano Lett.* **2011**, *11*, 1098; d) C. Novo, A. M. Funston, A. K. Gooding, P. Mulvaney, *J. Am. Chem. Soc.* **2009**, *131*, 14664; e) C. Novo, A. M. Funston, P. Mulvaney, *Nat. Nano* **2008**, *3*, 598.

[9] a) L. Tian, J. J. Morrissey, R. Kattumenu, N. Gandra, E. D. Kharasch, S. Singamaneni, *Anal. Chem.* **2012**, *84*, 9928; b) S. Tadepalli, Z. Kuang, Q. Jiang, K.-K. Liu, M. A. Fisher, J. J. Morrissey, E. D. Kharasch, J. M. Slocik, R. R. Naik, S. Singamaneni, *Sci. Rep.* **2015**, *5*, 16206; c) L. Tian, S. Tadepalli, S. H. Park, K.-K. Liu, J. J. Morrissey, E. D. Kharasch, R. R. Naik, S. Singamaneni, *Biosens. Bioelectron.* **2014**, *59*, 208.

[10] C. Wang, S. Tadepalli, J. Luan, K.-K. Liu, J. J. Morrissey, E. D. Kharasch, R. R. Naik, S. Singamaneni, *Adv. Mater.* **2017**, *29*, 1604433.

[11] S. Paz, J. C. Semenza, *Lancet* **2016**, *387*, 745.

[12] L. Tian, E. Chen, N. Gandra, A. Abbas, S. Singamaneni, *Langmuir* **2012**, *28*, 17435.

[13] C. Wang, J. Luan, S. Tadepalli, K.-K. Liu, J. J. Morrissey, E. D. Kharasch, R. R. Naik, S. Singamaneni, *ACS Appl. Mater. Interfaces* **2016**, *8*, 26493.

[14] H. Hakkinen, *Nat. Chem.* **2012**, *4*, 443.

[15] a) K.-S. Lee, M. A. El-Sayed, *J. Phys. Chem. B* **2005**, *109*, 20331; b) C. J. Orendorff, L. Gearheart, N. R. Jana, C. J. Murphy, *Phys. Chem. Chem. Phys.* **2006**, *8*, 165; c) H. Chen, L. Shao, Q. Li, J. Wang, *Chem. Soc. Rev.* **2013**, *42*, 2679.